A&A 591, A101 (2016)
DOI: 10.1051/0004-6361/201628383

Astronomy & Astrophysics

Different twins in the millisecond pulsar recycling scenario: Optical polarimetry of PSR J1023+0038 and XSS J12270-4859⋆,⋆⋆

M. C. Baglio[1,2], P. D'Avanzo[2], S. Campana[2], F. Coti Zelati[1,3,2], S. Covino[2], and D. M. Russell[4]

[1] Università dell'Insubria, Dipartimento di Scienza e Alta Tecnologia, via Valleggio 11, 22100 Como, Italy
e-mail: cristina.baglio@brera.inaf.it
[2] INAF, Osservatorio Astronomico di Brera, via E. Bianchi 46, 23807 Merate (LC), Italy
[3] Anton Pannekoek Institute for Astronomy, University of Amsterdam, Postbus 94249, 1090-GE Amsterdam, The Netherlands
[4] New York University Abu Dhabi, PO Box 129188, Abu Dhabi, United Arab Emirates

Received 25 February 2016 / Accepted 30 April 2016

ABSTRACT

We present the first optical polarimetric study of the two transitional pulsars PSR J1023+0038 and XSS J12270-4859. This work is focused on the search for intrinsically linearly polarised optical emission from the two systems. To this aim, we carried out multiband optical (*BVRi*) and near-infrared (NIR; *JHK*) photo-polarimetric observations of the two systems using the ESO New Technology Telescope (NTT) at La Silla (Chile), equipped with the EFOSC2 and the SOFI instruments. The system XSS J12270-4859 was observed during its radio-pulsar state; we did not detect a significant degree of polarisation in any of the bands, with 3σ upper limits, for example, of 1.4% in the *R*-band. We built the NIR−optical averaged spectral energy distribution (SED) of the system, which could be described well by an irradiated black body with radius $R_* = 0.33 \pm 0.03\,R_\odot$ and albedo $\eta = 0.32 \pm 0.05$, without the need for further components. Thus, we excluded the visible presence of an extended accretion disc and/or of relativistic jets. The case was different for PSR J1023+0038, which was in its accretion phase during our campaign. We measured a linear polarisation of $1.09 \pm 0.27\%$ and $0.90 \pm 0.17\%$ in the *V* and *R* bands, respectively. The phase-resolved polarimetric curve of the source in the *R* band reveals a hint of a sinusoidal modulation at the source 4.75 h orbital period, peaked at the same orbital phase as the light curve. The measured optical polarisation of PSR J1023+0038 could, in principle, be interpreted as electron scattering with free electrons, which can be found in the accretion disc of the system or even in the hot corona that sorrounds the disc itself, or as synchrotron emission from a jet of relativistic particles or an outflow. However, the NIR-optical SED of the system built from our dataset did not suggest the presence of a jet. We conclude that the optical linear polarisation observed for PSR J1023+0038 is possibly due to Thomson scattering with electrons in the disc, as is also suggested from the possible modulation of the *R*-band linear polarisation at the system orbital period.

Key words. stars: neutron – polarization – X-rays: binaries – stars: jets

1. Introduction

For years, millisecond radio pulsars (MSPs) have been believed to be the descendants of old, weakly magnetised neutron stars (NSs) that are hosted in low-mass X-ray binaries (LMXBs). The transfer of angular momentum from the low-mass companion to the NS through accretion is in fact considered possibly responsible for the spin-up of slow NSs in millisecond spinning sources (Alpar et al. 1982; Radhakrishnan & Srinivasan 1982). The initial NS, after switching off its radio pulsations while entering the so-called pulsar graveyard, might be re-accelerated through accretion and switch on again as a recycled MSP once the mass transfer is over (this is the so-called recycling scenario of MSPs; Srinivasan 2010). During the accretion phase, X-ray pulsations at the spin frequency might be detected. In this case, the system takes on the typical features of an accreting millisecond X-ray pulsar (AMXP). Fifteen AMXPs have been discovered so far (Patruno & Watts 2012).

The recycling scenario of MSPs discussed above was initially confirmed by the so-called "missing link pulsar", PSR J1023+0038 (Archibald et al. 2009), which was the first source that showed the potential to alternate between a radio pulsar phase with an X-ray state that is powered by accretion. Because of the repeated transitions that systems such as PSR J1023+0038 undergo from an accretion state to a rotation powered state, they are often referred to as transitional MSPs.

After decades of searching, however, the first direct observational evidence of the link between MSPs and NS-LMXBs has been found thanks to the detection of transient millisecond X-ray pulsations during an X-ray outburst from the transient LMXB IGR J18245−2452 that lasted a few weeks (Papitto et al. 2013); this was followed a few weeks later by the detection of a radio MSP. A similar system is the LMXB XSS J12270−4859. In recent years, radio, optical, and X-ray observations of this system suggested that, since the end of 2012, it may have switched to a MSP phase (Bassa et al. 2014; Bogdanov et al. 2014; de Martino et al. 2015), and the detection of 1.69 ms radio pulsations provided compelling evidence for the change of state (Roy et al. 2014).

Optical and infrared observations of such systems are frequently performed with both imaging and spectroscopic techniques. Most of the emission at these wavelengths is expected to

⋆ Based on observations made with European Southern Observatory (ESO) Telescopes at the La Silla Observatory under programme ID 094.D-0692(A), (B).
⋆⋆ The polarization table is only available at the CDS via anonymous ftp to cdsarc.u-strasbg.fr (130.79.128.5) or via http://cdsarc.u-strasbg.fr/viz-bin/qcat?J/A+A/591/A101

originate from the accretion disc that surrounds the NS or from the companion star. In particular, observations during quiescence offer a unique possibility to study the properties and characteristics of the companion star. Less used, but equally interesting, are optical and infrared linear polarimetric studies of LMXBs. The emission from these objects may, in fact, be polarised for different reasons, some of which are intrinsic to the sources. A first possible cause of linear polarisation lies in the accretion discs of LMXBs, which are heated from the compact object X-ray emission, causing the hydrogen to be almost completely ionised. In these conditions, electron scattering of radiation (initially emitted unpolarised) can occur in the geometrically symmetrical accretion disc, resulting in linearly polarised radiation at a constant level. Any phase-dependent variations may be due to asymmetries in the disc geometry or system configuration. However, each electron that is responsible for the scattering in the disc oscillates in principle in a random direction. Therefore, the large amount of expected linear polarisation caused by electron scattering never exceeds a few per cent in the optical and infrared bands for LMXBs owing to strong cancellation effects. An alternative and intriguing scenario links the detection of linear polarisation in LMXBs to the possible emission of a relativistic particle jet, which is similar to what occurs in active galactic nuclei. The radiation emitted from a leptonic jet has a synchrotron nature, which is known to be intrinsically linearly polarised up to tens of per cent. Even in this case, because of the presence of strongly tangled magnetic fields in the jet, radiation is expected to be polarised at a few per cent at most, mainly at lower frequencies (the radio and infrared bands; Russell & Fender 2008).

2. Targets of this work

2.1. PSR J1023+0038

The first system that showed the potential to alternate its radio pulsar phase, powered by rotation, to an X-ray phase, powered by accretion, was the 1.69 ms radio pulsar in a 4.75 h binary orbit PSR J1023+0038 (hereafter J1023). This system was discovered by Bond et al. (2002) in the radio band and was initially classified as a magnetic cataclysmic variable. Optical studies revealed signs for the presence of an accretion disc in 2001 (Szkody et al. 2003), which led to identify it as a NS−LMXB. No enhanced X-ray emission was reported. In 2007, a 1.69 ms radio pulsar was discovered to be the compact object of the system (Archibald et al. 2013). J1023 underwent a state change from the MSP state to an accretion-disc dominated state in June 2013, with a consequent switch off of the radio pulsed signal and a significant increase in the GeV flux (Stappers et al. 2014).

The system has been the subject of extensive multi-wavelength campaigns after its change of state (Halpern et al. 2013; Kong 2013; Linares et al. 2014; Patruno et al. 2014; Takata et al. 2014; Tendulkar et al. 2014; Coti Zelati et al. 2014; Deller et al. 2015; Archibald et al. 2015; Bogdanov et al. 2015; Shahbaz et al. 2015). Radio band observations performed by Deller et al. (2015), in particular, showed a rapidly variable and flat spectrum that persisted over six months.

During the multi-wavelength observational campaign reported in Bogdanov et al. (2015), the system was observed to exhibit short-lived, but frequent and stable episodes of mode switching in the X-rays (factor of ∼6 in flux), occurring on timescales of ∼10 s. In the UV and optical, Bogdanov et al. (2015) reported on occasional intense flares that were coincident with those observed in the X-rays. Radio observations revealed no pulsations at the pulsar period during any of the three X-ray modes, which is probably due to the quenching/screening of radio emission mechanisms by the accretion flow. Shahbaz et al. (2015) reported on an optical campaign performed on J1023 with the *William Herschel* Telescope (WHT) and the Telescopio Nazionale *Galileo* (TNG) telescopes. The highest time-resolution (0.31 and 0.97 or 3.37 s respectively) light curves showed, for the first time, the presence of rectangular dip features randomly distributed with the orbital phase, which are similar to the mode-switching behaviours observed in the X-ray light curves of the source.

The companion star of the system was spectroscopically classified as a *G*-type star (moderately irradiated by the compact object) and has a mass of $\sim 0.2\,M_{\odot}$ (Archibald et al. 2009). The distance of the system is 1.37 kpc (Deller et al. 2012), from which the authors derived an estimate of the mass of the pulsar ($1.71 \pm 0.16\,M_{\odot}$). Finally, Archibald et al. (2013) evaluated the system inclination as $42^{\circ} \pm 2^{\circ}$.

2.2. XSS J12270-4859

Discovered by the Rossi X-ray Timing Explorer (Sazonov & Revnivtsev 2004), XSS J12270−4859 (hereafter J12270) was initially classified as a cataclysmic variable hosting a magnetic white dwarf (Masetti et al. 2006; Butters et al. 2008) based on the presence of optical emission lines. Subsequent independent multi-wavelength studies (Pretorius 2009; Saitou et al. 2009; de Martino et al. 2010, 2013; Hill et al. 2011; Papitto et al. 2015) casted doubts on this classification, suggesting instead an identification as a LMXB showing unusual dipping and flaring behaviour on timescales of few hundreds of seconds. XSS J12270−4859 was subsequently recognised to be spatially coincident with a moderately bright gamma-ray source that was detected by *Fermi*-LAT emitting up to 10 GeV (de Martino et al. 2010; Hill et al. 2011), and is now known as 3FGL J1227.9−4854.

The system remained stable in gamma rays, X-rays, and optical wavelengths for about a decade until 2012 November/December, when a substantial decline in brightness in all of these bands was reported (Bassa et al. 2013; Tam et al. 2013; Bassa et al. 2014; Bogdanov et al. 2014). This variability reinforced the prediction, first made by Hill et al. (2011), that the system could harbour an active radio MSP, sharing similar properties with J1023. Follow-up observations in the radio finally succeeded in detecting pulsations at a period of 1.69 ms (Roy et al. 2014).

The orbital period of the system is 6.91 h (Bassa et al. 2014; de Martino et al. 2014) and the companion is a G5-type, donor star with a mass of $0.15-0.36\,M_{\odot}$ (de Martino et al. 2014), which dominates the UV/optical and near-IR (NIR) emissions. The distance is estimated to be about 1.4 kpc, and the analysis of optical light curves constrains the binary inclination in the $46^{\circ} \lesssim i \lesssim 65^{\circ}$ interval (de Martino et al. 2015).

3. Optical polarimetry with EFOSC2

The systems J1023 and J12270 were observed in quiescence on 8 and 9 February 2015 (respectively) with the ESO New Technology Telescope (NTT), located at La Silla (Chile), equipped with the EFOSC2 camera in polarimetric mode and using *B*, *V*, *R*, *i* filters. The night was photometric, with seeing constant at a level of $\sim 0.6-0.8''$, and the Moon at 84%. We performed image reduction following the standard procedure of subtraction of

Table 1. Complete log of the NTT optical observations performed on 8 February 2015.

Target	Filter	Exposure time (per pos angle)	UT mid observation (YYYmmdd)
J1023	*B*	5 × 60 s	20150208.2898
	V	5 × 60 s	20150208.2944
	R	5 × 60 s	20150208.2990
	i	5 × 60 s	20150208.3036
J12270	*B*	4 × 120 s	20150209.2110
	V	4 × 120 s	20150209.2184
	R	4 × 120 s	20150209.2257
	i	4 × 120 s	20150209.2330

an average bias frame and division by a normalised flat frame. We performed the flux measurements using aperture photometry techniques on the fields of the two targets with `daophot` (Stetson 1987). A Wollaston prism was inserted in the path of radiation to obtain polarimetric observations. In this way, the incident radiation was split into two beams, with orthogonal polarisation, called ordinary (*o*-) and extraordinary (*e*-) beams. A mask allowed the different beams not to overlap on the CCD. The instrument was also equipped with a rotating half wave plate (HWP), which is able to rotate the polarisation plane of the incident radiation in a direction that is symmetrical to its optical axis. In particular, the linear polarisation direction of the radiation exiting the plate rotates at double velocity with respect to the angular velocity of the plate itself.

The linear polarisation (LP) of radiation is entirely described by the Stokes parameters Q and U, defined as follows:

$$Q = f^o(0°) - f^e(0°); \qquad U = f^o(45°) - f^e(45°), \tag{1}$$

where $f^o(0)$, $f^e(0)$, $f(^o45)$, $f^e(45)$ are the ordinary (o) and extraordinary (e) fluxes of the linearly polarised components at 0° and 45° degrees, respectively (angles are intended with respect to the telescope axis). To obtain an estimate of Q and U, it would thus be enough to take two images (with the Wollaston prism mounted on the instrument) at the position angles $\Phi = 0°$ and 45°, for example, by rotating the whole instrument by the two angles with respect to the telescope axis. Images at four different angles (i.e. $\Phi = 0°, 45°, 90°, 135°$) are often taken, however, to increase the precision of the polarimetric measurement. Since EFOSC2 is equipped with a HWP that can rotate, it is also possible to avoid rotating the whole instrument; for this reason, images were taken at the four angles of the HWP rotator, $\Phi_i = 22.5° (i-1), i = 1, 2, 3, 4$, which correspond to a rotation of the instrument by $\Phi = 0°, 45°, 90°, 135°$, respectively.

Alternating the filters, we obtained a set of five 60 s integration images and four 120 s integration images for the targets J1023 and J12270, respectively, for each filter and HWP angle (a log of the optical observations is reported in Table 1).

In this configuration, Eq. (1) for deriving Q and U translates into the following equations for the normalised Stokes parameters (a precise derivation is found in di Serego Alighieri 1998; Tinbergen 1996 and Schmid 2008):

$$Q = \frac{F(\Phi_1) - F(\Phi_3)}{2}; \quad U = \frac{F(\Phi_2) - F(\Phi_4)}{2}, \tag{2}$$

where

$$F(\Phi_i) = \frac{f^o(\Phi_i) - f^e(\Phi_i)}{f^o(\Phi_i) + f^e(\Phi_i)}, \tag{3}$$

and $f^o(\Phi_i)$, $f^e(\Phi_i)$ are the ordinary (o) and extraordinary (e) fluxes observed with the HWP rotator oriented at $\Phi_i = 22.5°(i-1), i = 1, 2, 3, 4$.

Once the Stokes parameters are worked out, it is possible to obtain an estimate of the LP degree simply by computing the quantity

$$P = \sqrt{Q^2 + U^2}. \tag{4}$$

This simple expression, however, does not takes into account either possible LP induced by the interaction of the radiation emitted by our targets with interstellar dust along the line of sight, or any possible instrumental effect that could induce the polarisation of the light; for example the reflection on the 45° mirror of the telescope, which introduces strong instrumental effects when the telescope has a Nasmyth focus, as in the case of the NTT). For low polarisation levels, one possibility is to correct the values of Q and U of the targets obtained, as described above, using the Stokes parameters of an unpolarised standard star (or the weighted mean of the Stokes parameters evaluated for a group of field stars that are supposed to be unpolarised). In addition, since the Stokes parameter statistics is not Gaussian (Wardle & Kronberg 1974; di Serego Alighieri 1998), the LP degree obtained with Eq. (4) after the correction of Q and U must be, in turn, corrected for a bias factor as described by the following equation:

$$P = P_{\rm obs}\sqrt{1 - \left(\frac{\sigma_{\rm P}}{P_{\rm obs}}\right)^2}, \tag{5}$$

where $P_{\rm obs}$ and $\sigma_{\rm P}$ are the LP degree obtained with Eq. (4) and the rms error on the LP degree, respectively.

Alternatively, one could compute, for each value of the instrumental position angle Φ, the quantity

$$S(\Phi) = \left(\frac{f^o(\Phi)/f^e(\Phi)}{\langle f^o_u(\Phi)/f^e_u(\Phi_i)\rangle} - 1\right) \Big/ \left(\frac{f^o(\Phi)/f^e(\Phi)}{\langle f^o_u(\Phi)/f^e_u(\Phi)\rangle} + 1\right), \tag{6}$$

where $\langle f^o_u(\Phi)/f^e_u(\Phi)\rangle$ is the averaged ratio between the ordinary and extraordinary fluxes of the unpolarised field stars (chosen as reference), which are supposed to be subject to the same extinction as the target itself. As exhaustively described in di Serego Alighieri (1998), this parameter gives an estimate of the projection of the LP along the different directions. The parameters S and the LP degree and angle (P and $\theta_{\rm P}$, respectively) are then related through the relation

$$S(\Phi) = A + P\cos 2(\theta_{\rm P} - \Phi), \tag{7}$$

where A is a constant. The fit of $S(\Phi)$ with Eq. (7) yields P from the semi-amplitude of the oscillation and θ_P from the position of the first maximum of the curve. From the constant A, the presence of a residual interstellar or instrumental component to the LP is proven.

The S parameter is already normalised to the non-polarised reference stars; in this way, it is guaranteed to obtain values of P that are automatically corrected both for interstellar and instrumental effects. In case any residual effect is present, it would be simply indicated by the observation of a shift with respect to 0 along the y-axis of the sinusoidal function reported in Eq. (7). Moreover, with this method no bias correction (Eq. (5)) due to the non-Gaussianity of the polarisation measurement is needed if we apply proper techniques to derive confidence intervals in multi-parametric fits.

4. Near-infrared polarimetry with SOFI

The systems J1023 and J12270 were observed on 7 February 2015 in photo-polarimetric mode with the NTT equipped with the SOFI instrument in the NIR (J, H, K bands). The night was clear, with seeing ~0.8″ during the whole night. To obtain a precise illumination correction[1] of our frames, we performed image reduction by subtracting an average dark frame and dividing by a normalised special flat frame that was obtained through a `midas` procedure available on the ESO website[2]. All of the flux measurements were performed with the `daophot` task, as for the optical (Sect. 3). Even in SOFI, a Wollaston prism guarantees the split of incident radiation in the two orthogonally polarised o- and e-beams. As in the case of EFOSC2, a mask prevents any overlapping of the two beams. Nevertheless, a rotating HWP is not provided in this instrument. For this reason, it is necessary to rotate the whole instrument cyclically with respect to the telescope axis, with an angle $\phi_i = 45°(i-1)$ where $i = 1, 2, 3, 4$, to obtain the images at different angles needed to perform a LP measurement. In this way, the observed field always appears different between an image and its consecutive that is rotated of 45° with respect to the previous image. Because of this, unless the observed field is particularly crowded (that is not the case of our two targets), in the infrared it is difficult to obtain a group of (or even one) field stars that can be imaged for each orientation of the instrument, and that can be used as reference unpolarised stars to correct the Stokes parameters of the target for interstellar and instrumental effects. Moreover, because of the Nasmyth focus of the instrument, the entity of these effects depends on the direction of the observation and, for this reason, one needs to observe objects that are exactly at the same azimuth of the targets to obtain a precise correction (this would be the case of the reference field stars, if present) or to implement a model that is able to take into account all of the possible instrumental contaminations of the polarimetric measurements. A similar model was implemented for the PAOLO instrument mounted at the TNG (Covino et al. 2014). This model is currently under construction and the SOFI polarimetric images remain thus still uncalibrated.

5. Results

5.1. NIR and optical imaging of J1023 and J12270

The photo-polarimetric images of J1023 and J12270 allowed us to extract their optical-NIR fluxes. While in the NIR we summed together all of the images to enhance the signal-to-noise ratio of the observations, in the case of the optical images we built the *BVRi* light curves of the system. We computed the total flux of each star in the two fields simply by summing the intensities of the ordinary and extraordinary beams in all of the collected images (see Sects. 3 and 4 for details on the flux measurements). We then performed differential photometry, with respect to a selection of isolated field stars, with the aim of minimising any systematic effect. Finally we calibrated the infrared magnitudes using the 2MASS[3] catalogue, the optical magnitudes of J1023 using the SDSS[4] catalogue, and the optical magnitudes of J12270 using the APASS[5] catalogue; we used the transformation equations of Jordi et al. (2006) to pass from the SDSS and APASS *gri* magnitudes to the *BVR* Johnson−Cousin magnitudes. The optical light curves of the two sources can all be fitted with sinusoidal functions that are modulated at the known orbital periods of the systems (4.75 h and 6.9 h for J1023 and J12270, respectively). The results of the NIR and optical photometry of J1023 and J12270, together with the results of the sinusoidal fits in the optical are reported in Table 2 and are shown in Figs. 1 and 2.

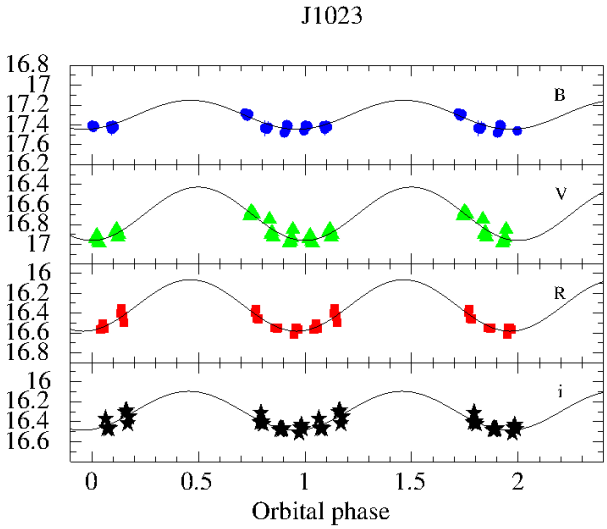

Fig. 1. *From top to bottom*, *BVRi* light curves (magnitudes vs. orbital phase) of J1023. Magnitudes are not corrected for reddening. The sinusoidal fits of the curves with period fixed to 1 are superimposed. Errors are indicated at the 68% confidence level. Two periods are drawn for clarity.

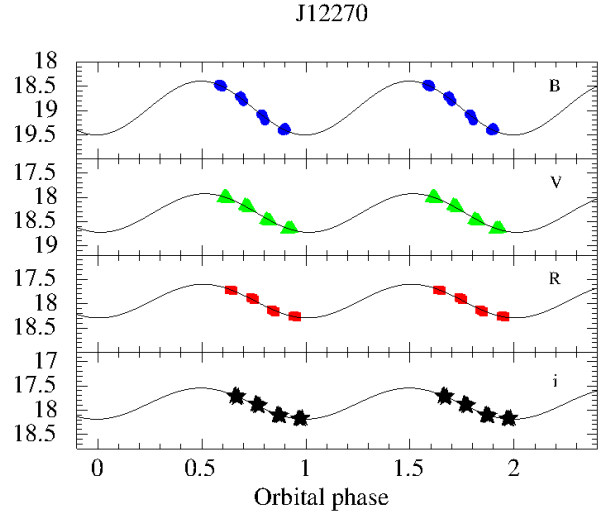

Fig. 2. *From top to bottom*, *BVRi* light curves (magnitudes vs. orbital phase) of J12270. Magnitudes are not corrected for reddening. The sinusoidal fits of the curves with period fixed to 1 are superimposed. Errors are indicated at the 68% confidence level. Two periods are drawn for clarity.

5.2. Optical polarimetry of PSR J1023+0038

With the aim of enhancing the signal-to-noise ratio (S/N) of the observation, we first of summed together the five images in each optical band. Starting from the results of aperture photometry performed on the stars of the field, we applied the method

[1] https://www.eso.org/sci/facilities/lasilla/instruments/sofi/tools/reduction/flat_fielding.html
[2] https://www.eso.org/sci/facilities/lasilla/instruments/sofi/tools/sofi_scripts.html
[3] http://www.ipac.caltech.edu/2mass/
[4] http://www.sdss3.org/dr10
[5] https://www.aavso.org/download-apass-data

Table 2. Results of NIR and optical photometry performed on J1023 and J12270.

Filter	Frequency (Hz)	Semi-amplitude (mag)	Maximum (phase)	Mean magnitude	χ^2/d.o.f.	A_λ (mag)
			J1023			
J	2.41×10^{14}	–	–	15.23 ± 0.03	–	0.076 ± 0.009
H	1.81×10^{14}	–	–	14.98 ± 0.04	–	0.049 ± 0.006
K	1.39×10^{14}	–	–	14.45 ± 0.06	–	0.033 ± 0.004
i	3.78×10^{14}	0.19 ± 0.02	0.45 ± 0.01	16.29 ± 0.02	120.00/17	0.17 ± 0.02
R	4.67×10^{14}	0.26 ± 0.02	0.46 ± 0.01	16.32 ± 0.01	131.80/17	0.23 ± 0.03
V	5.48×10^{14}	0.27 ± 0.01	0.50 ± 0.01	16.69 ± 0.01	232.20/17	0.29 ± 0.03
B	6.82×10^{14}	0.15 ± 0.03	0.46 ± 0.02	17.30 ± 0.03	27.46/17	0.38 ± 0.05
			J12270			
J	2.41×10^{14}	–	–	16.94 ± 0.06	–	0.093 ± 0.003
H	1.81×10^{14}	–	–	16.63 ± 0.11	–	0.060 ± 0.002
K	1.39×10^{14}	–	–	16.21 ± 0.21	–	0.041 ± 0.001
i	3.78×10^{14}	0.32 ± 0.08	0.49 ± 0.06	17.87 ± 0.15	0.58/13	0.20 ± 0.01
R	4.67×10^{14}	0.34 ± 0.03	0.51 ± 0.03	17.95 ± 0.05	5.00/13	0.28 ± 0.01
V	4.66×10^{14}	0.40 ± 0.02	0.48 ± 0.03	18.32 ± 0.05	5.00/13	0.36 ± 0.01
B	6.82×10^{14}	0.55 ± 0.05	0.50 ± 0.05	18.95 ± 0.13	1.72/13	0.47 ± 0.02

Notes. The magnitude values (Vega magnitudes for the *JHKBVR* filters; AB magnitudes for the i filter) are not corrected for reddening, the parameters of which are reported in the last column (the A_V has been derived from Schlafly & Finkbeiner 2011, for J12270 and from the $N_{\rm H} = 5.3 \times 10^{20}$ cm^{-2} estimate reported in Campana et al., in prep. for J1023). In the 6th column, the reduced χ^2 of the sinusoidal fits of the optical light curves are reported.

described in Sect. 3 to evaluate the degree of LP, passing by the fit of the S parameter (Eq. (6)) with the function reported in Eq. (7). The results are tabulated in Table 3.

If we set the minimum significance needed to define a detection of LP at a 3σ level, we obtain evidence of polarised emission just in V- and R-bands, where the first is slightly higher than the latter. Since our measurements are consistent in the B- and i-bands with zero at the 2.3σ and 2.5σ confidence level, respectively, we were able to evaluate the 3σ upper limits to the LP; these are reported in Table 3. In contrast to what occurs in the B-band, the i-band upper limit is particularly constraining, suggesting that the LP degree gets lower and lower while moving to longer wavelengths. The B-band polarisation measurement instead has a high uncertainty as a result of the presence of a full moon, the radiation of which is polarised due to reflection; this affects any LP optical measurement above all at higher frequencies (i.e. the B-band).

We then tried to search for any possible phase-dependent variation of the optical LP of J1023. To this aim, we analysed each of the five datasets for each band separately, so that we could ascertain the trend of the degree of polarisation with respect to the orbital phase in the four bands; the phase was obtained starting from the ephemeris reported in Archibald et al. (2009).

In some cases, the S/Ns of the single observations in the B- and i-bands were not high enough to permit even a 1σ significance detection of LP. Therefore, we could not detect any possible variations of LP with the orbital phase of the system. In the R- and V-bands, we obtained $>1\sigma$ detections of LP in almost all of the datasets, in particular, in the R-band, where the significance of each measurement is always $>2.3\sigma$ and exceeds 3σ in one case. While the polarisation trend seems to be almost constant with the orbital phase in the V-band (Fig. 3, bottom panel; excluding the upper limits, a constant fit of the remaining points yields χ^2/d.o.f. = 0.3/3), the curve clearly deviates from constant in the R-band (the fit with a constant yields χ^2/d.o.f. = 7.32/4). In particular, the shape of the polarisation curve seems to suggest a sinusoidal trend (Fig. 4, bottom panel). The fit with a sinusoidal function with a period fixed to the orbital period of J1023 (4.75 h) gives an acceptable χ^2/d.o.f. (0.11/2). Moreover, it is interesting to compare the R-band light curve with the polarisation curve in this band. The positions of the maxima of the two curves are both located around phase 0.5 (superior conjunction of the companion star, i.e. when the observer sees the irradiated face of the donor), as the two positions are consistent with each other within 1σ (maximum of the light curve phase: 0.46 ± 0.01; maximum of the polarisation curve phase: 0.57 ± 0.13; errors at the 68% confidence level). The fit of the R-band polarisation curve with a constant model is still preferable to the constant plus sinusoidal model, despite the high χ^2/d.o.f. of the former; according to an F-test, the addition of a sinusoidal function gives a probability of $\sim 1.5 \times 10^{-2}$, corresponding only to a marginal 2.6σ improvement in the fit. Nevertheless, an intriguing increase of the degree of polarisation towards phase 0.5 is clearly observed (Fig. 4).

Table 3. Results of the optical polarimetry performed on J1023.

B	V	R	i
	P (%)		
1.17 ± 0.51	1.09 ± 0.27	0.90 ± 0.17	0.55 ± 0.22
	P (3σ upper limit)		
2.7%	–	–	1.21%
	Interstellar/instrumental LP (3σ upper limit)		
1.23%	0.63%	0.48%	0.54%

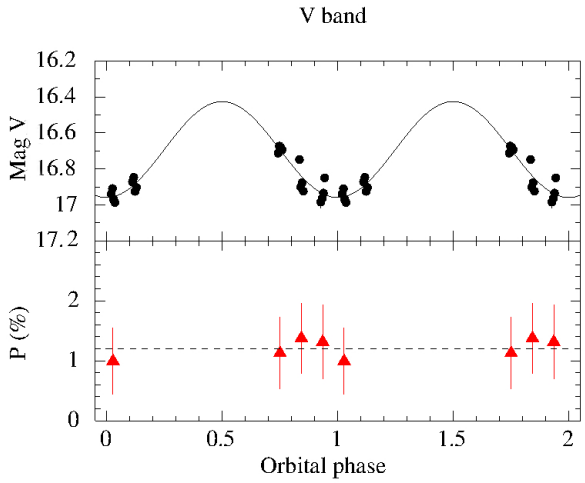

Fig. 3. *Upper panel*: V-band light curve of J1023 (magnitude vs. orbital phase). The solid line represents the fit of the light curve with a sinusoidal function with period fixed to 1 (corresponding to 4.75 h; Archibald et al. 2009). *Bottom panel*: V-band polarisation curve represented as a function of the orbital phase of the system. The $>1\sigma$ detections are represented with red triangles, whereas we indicated the 3σ upper limits with red arrows, where necessary. The fit of the $>1\sigma$ detections with a constant function is superimposed (dashed line; χ^2/d.o.f. $= 0.28/3$). Errors are represented at the 68% confidence level. Two periods are drawn for clarity.

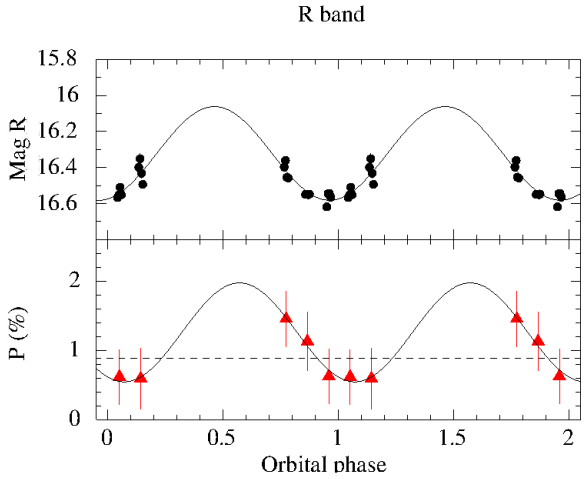

Fig. 4. *Upper panel*: R-band light curve of J1023 (magnitude vs. orbital phase). With a solid line, a fit of the light curve with a sinusoidal function with period fixed to 1 (corresponding to 4.75 h; Archibald et al. 2009) is reported. The χ^2/d.o.f. of the fit is 11.35/17. *Bottom panel*: R-band polarisation curve represented with respect to the orbital phase of the system. The fits with a constant function (dashed line; χ^2/d.o.f. $= 3.66/4$) and with a sinusoidal function with period fixed to 1 are superimposed (solid line; χ^2/d.o.f. $= 0.11/2$). Errors are represented at the 68% confidence level. Two periods are drawn for clarity.

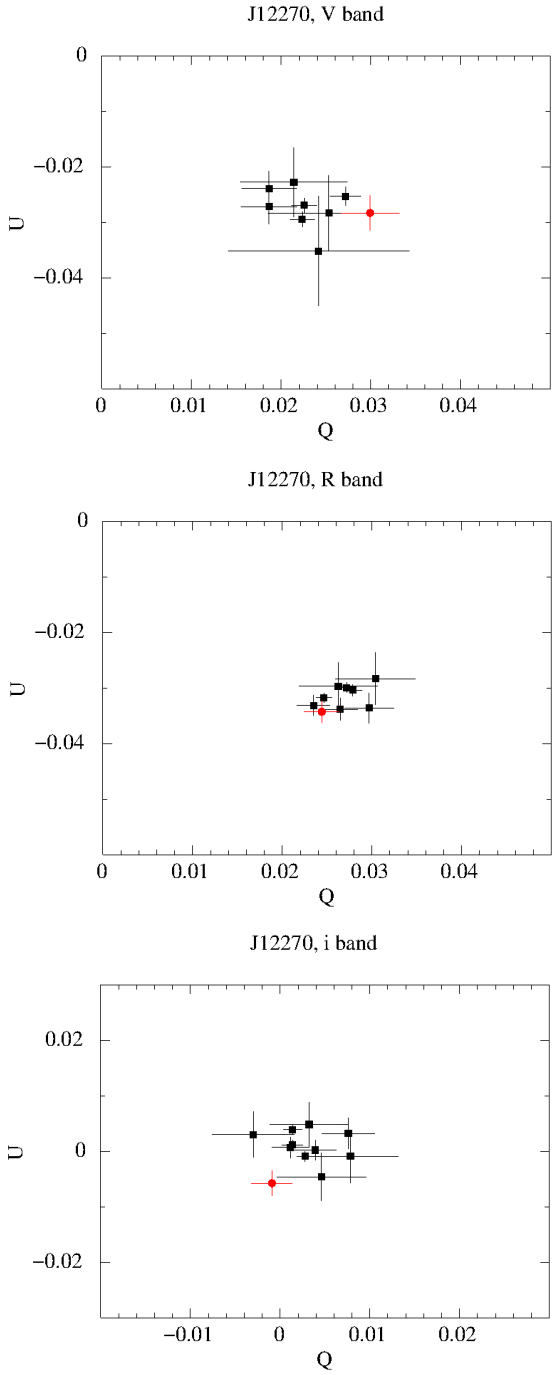

Fig. 5. *From top to bottom*: U vs. Q for the averaged images in the optical VRi filters for J12270 (red dot) and a group of reference field stars (black squares). The reference stars and target cluster around a common value in all of the bands, which testifies that J12270 is probably not intrinsically linearly polarised.

5.3. Optical polarimetry of XSS J12270-4859

Following the same procedure performed on J1023, we averaged all of the images collected in each optical band for J12270 to enhance the S/N and to evaluate the average optical LP of the target. As a first step, we managed to estimate the Stokes parameters, Q and U, (Eq. (2)) of J12270 and of a group of comparison stars in the same field of the target that were supposed to be unpolarised. The results are shown in Fig. 5 for the V, R, and i-band, where the Stokes parameters are represented in the $Q-U$ plane for each filter. Because of the effect of the Moon, the Stokes parameters in the B-band were too dispersed to faciliate such a study. As shown in the figure, the Stokes parameters of the reference stars cluster very well around common values in each plot; these values represent the corrections that one has to apply in each band to the Stokes parameters of the target to eliminate all of the possible interstellar and instrumental contributions to the LP of its emitted radiation. This clustering confirms that the objects chosen as reference are indeed intrinsically not polarised (if they were, they would act independently of each other and

Table 4. Results of the optical polarimetry performed on J12270.

B	V	R	i
	P (%)		
1.77 ± 1.33	0.73 ± 0.59	0.40 ± 0.34	0.74 ± 0.41
	P (3σ upper limit)		
5.76%	2.50%	1.42%	1.97%
	Interstellar/instrumental LP (3σ upper limit)		
3.30%	1.27%	0.93%	1.45%

Notes. In particular, the LP degree corresponds to the semi-amplitude of the sinusoidal function used for the fit of the S parameter, reported in Eq. (6), whereas the residual interstellar and instrumental polarisation is indeed obtained as the constant parameter of the same fit.

no clustering would be present). The fact that the target might show different behaviour in the $Q - U$ plane with respect to the unpolarised reference stars could be the first hint of the possible intrinsic LP of its radiation. As clearly visible in Fig. 5, this is not the case for J12270.

We then continued the analysis by evaluating the S parameter of J12270 at the different angles Φ (Eq. (6)). Since the field of the target is sufficiently crowded, we used the o- and e-fluxes of the group of reference stars in Eq. (6). The results of the fit of $S(\Phi)$ with Eq. (6) are tabulated in Table 4.

As can be observed in Table 4, the significance of our findings is below 2σ in all of the bands. We could thereby evaluate 3σ upper limits to the optical LP of the target, which are reported in Table 4 together with the upper limits to the possible residual interstellar and instrumental polarisation derived from the S parameter fit with Eq. (7).

We tried to search for possible variations of the LP with the orbital phase of the system because it is possible that in the process of averaging all of the collected images at different orbital phases some cancellation effects came to pass. A $\geqslant 1\sigma$ polarisation detection, however, was not possible in any of the analysed epochs.

6. Discussion

6.1. Thomson scattering induced LP

Unpolarised radiation emitted from an astrophysical source can be polarised from different physical phenomena. The most frequent among these phenomena is electron scattering (Thomson scattering), according to which a free electron with a certain oscillation direction absorbs the incident, unpolarised radiation and re-emits it as linearly polarised in the same direction of its oscillation. Thomson scattering in an astrophysical scenario can take place in different cases. The most common is the interaction of radiation with free electrons in the interstellar medium that can be found along the line of sight between the source of radiation and the observer. In this case, the induced polarisation has been demonstrated to have a precise wavelength dependency following the so-called Serkowski law (Serkowski et al. 1975). In general, a rough estimate of the maximum expected interstellar contribution to the interstellar polarisation can be derived simply with the empirical formula (Serkowski et al. 1975),

$$P_{\rm int,max} \leqslant 3A_V, \tag{8}$$

where A_V is the absorption coefficient of the target in analysis in the optical V-band. In the case of LMXBs, this contribution

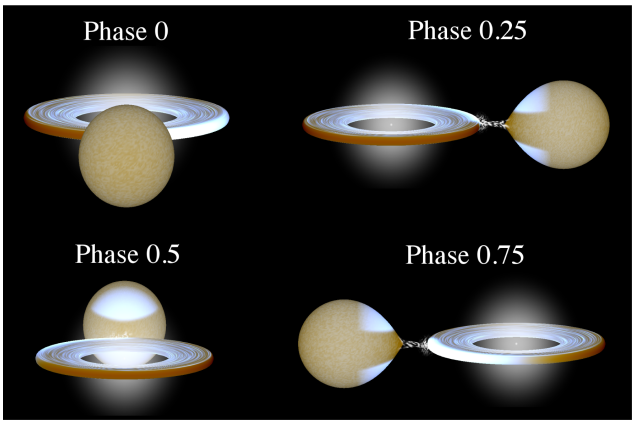

Fig. 6. Representation of a LMXB with the same orbital period of J1023 (4.75 h) and a fictitious inclination $i = 80°$, as seen from an external observer, obtained with the *BinSim* software (available at http://www.phys.lsu.edu/~rih/binsim/). The four principal orbital phases of the system are taken into account.

to the LP is usually treated as an effect to be corrected for to search for other more interesting (and possibly intrinsic to the source) polarising phenomena. In particular, for these sources and also in the field of polarisation induced by Thomson scattering, an intriguing possibility is that unpolarised light emitted from any system component (i.e. the companion star, the NS, and even the accretion disc) may interact with the free electrons in the ionised accretion disc itself. In this case, as shown in Brown et al. (1978) and Dolan (1984), the resulting LP degree should not exceed a few per cent in the optical because of cancellation effects. Moreover, the LP degree should not depend on wavelength. The polarisation spectrum is expected to reproduce the spectrum of the incident radiation because the Thomson cross section is known to be wavelength independent. Since the hot accretion disc is principally responsible for the scattering in LMXBs, the level of LP is expected to increase with frequency in the optical regime. On the other hand, the degree of polarisation due to Thomson scattering has a dependency on the scattering angle (di Serego Alighieri 1998) and, in the case of binary systems, on the inclination i of the binary orbit (Dolan 1984). Interestingly, in case LP is induced by Thomson scattering, the Stokes parameters Q and U and the LP degree are expected to have a sinusoidal dependency on the orbital phase of the system (Brown et al. 1978; Dolan & Tapia 1988; Dolan & Tapia 1989).

In the case of J1023, all of these considerations allow us to hypothesise that the measured LP (Table 3) may have its origin in the Thomson scattering of radiation with the free electrons in the accretion disc.

Possible evidence in favour of our hypothesis is the observation of the hinted tendency of the R-band polarisation curve to oscillate at the system 4.75 h orbital period (Fig. 4). In particular, it is interesting that the position of the LP maximum seems to coincide within the errors with that of the light curve, i.e. phase ~0.5. This corresponds to superior conjunction, when the observer sees the irradiated face of the companion star. In order to try to model what we observed qualitatively, we consider a LMXB with inclination $i \sim 90°$ for simplicity (Fig. 6). The optical radiation coming from such a system is the combination of the emission of the companion star and that of the accretion disc, as the X-ray emission of the internal disc is partially reprocessed by external radii.

When the companion star of the system is in phase of superior conjunction (phase 0.5, Fig. 6), the accretion disc is found

exactly along the line of sight between the observer and companion star, causing the radiation emitted from both the companion star and accretion disc to cross the accretion disc itself (if the latter is sufficiently extended and thick). In this way part of the radiation interacts with free electrons that can be found in the disc and in the disc corona via Thomson scattering, thus resulting in a linearly polarised emission. When the system is instead at inferior conjunction (phase 0 − when the observer sees the back side of the companion star), the optical radiation observed can again be ascribed to the same sources, even if the disc is partially shaded by the companion star. The configuration is now inverted, however, and the radiation emitted from the companion star is not intercepted by the accretion disc and the corona. This makes Thomson scattering of the photons (produced by the partially shaded accretion disc) with the free electrons in the disc and in the corona, responsible for the emission of polarised radiation. Hence, this implies a decrease in the LP of the total optical emitted light, as observed (Fig. 4). In the case of J1023, moreover, a propeller scenario was proposed to account for the X-ray emission observed during the accretor phase (Papitto & Torres 2015; Campana et al. in prep.), according to which part of the accreting material may be halted at the NS magnetosphere. In this way, many free electrons may enclose the system, which enhances the probability of Thomson scattering of the emitted photons (even if equally at all of the orbital phases).

Our simple, qualitative model could thus explain the variability of the *R*-band polarisation curve shown in Fig. 4. A good test bed for this hypothesis would be the observation of a similar, sinusoidal trend of the LP with the orbital phase in the other optical bands as well; this was unfortunately not allowed by our data (as shown in Fig. 3 for the *V*-band), which is probably due to a S/N that is too low and, at higher frequencies, to the contaminant presence of the full moon. Moreover, once the oscillation is confirmed, a full coverage of the orbital period would help to constrain some physical and geometrical properties of the system (see e.g. Gliozzi et al. 1998).

In contrast to the case of J1023, in the case of the LMXB J12270 we do not possess any LP 3σ over zero detection in the optical. This is however consistent with our hypothesis, according to which the LP of J1023 would be induced by Thomson scattering in the accretion disc of the system. In fact from previous works published on the transitional pulsar J1023 (e.g. Bogdanov et al. 2015, and references therein) we know that the source is in an accretion-disc dominated state since 2013, which means that an accretion disc is indeed present in the system and can therefore be the cause of the observed LP. On the contrary, J12270 has been lingering in a radio pulsar state since the end of 2012 (de Martino et al. 2015). In this condition, an accretion disc cannot be formed because the accreting material is wiped out from the radio emission of the pulsar. Consequently, the radiation emitted from J12270 is definitely not expected to be linearly polarised (or at least not because of Thomson scattering with electrons in an ionised accretion disc).

6.2. Other possible causes: jet of relativistic particles

An intriguing, possible origin of the linear polarisation in LMXBs is the production of jets of relativistic particles. Such phenomena emit synchrotron radiation, for instance, which is known to be intrinsically linearly polarised up to tens of per cent, depending on the level of ordering of the magnetic field at the base of the jet. Jets have been observed both in BH and NS LMXBs and, in the case of BH LMXBs, their coupling with the accretion state of the source has been extensively pointed out. In particular, accretion states associated with hard X-ray spectra appear to be linked to the production of a relatively steady, continuously replenished and partially self-absorbed outflow (Fender 2001), while major outbursts are associated with more discrete ejection events. In the radio band, the jets observed during the hard X-ray states of LMXBs have a flat spectrum. Above certain frequencies this flat spectral component breaks to an optically thin spectrum corresponding to the point at which the entire jet becomes transparent. There is evidence, both from some BH and NS X-ray binaries, that this break occurs around the NIR spectral region (e.g. Migliari et al. 2010; Gandhi et al. 2011). Thus there is a strong case for a significant contribution of synchrotron emission in the NIR-optical spectral regimes of LMXBs when a jet is emitted (Russell et al. 2011).

For most BH and NS LMXBs in which jets have been detected, the optical and NIR polarisation do not exceed a few per cent. This means that the magnetic fields at the base of the jets are usually strongly tangled (e.g. Schultz et al. 2004; Russell et al. 2011; Baglio et al. 2014b), and the only known exception to this is the system Cyg X−1, for which on the contrary an ordered magnetic field has been measured (Russell & Shahbaz 2014).

The X-ray luminosity of the two targets of this work, J1023 and J12270, is orders of magnitudes lower with respect to the NS LMXBs for which jets are usually inferred (Deller et al. 2015). However, Deller et al. (2015) found for J1023 a radio flux density and spectral index that were reminiscent of synchrotron emission due to a jet of relativistic particles. For this reason it is not possible to completely rule out the possibility that the optical LP measured for J1023 (Table 3) could be due to a jet. All of the upper limits and the detection of LP for J1023 (and for J12270 also), in fact, are sufficiently constraining enough to rule out this scenario. If we hypothesise that a jet was emitted in both sources, we can try to estimate its maximum contribution to the total *i*-band flux (that is the optical band in which the jet contribution should be stronger), following what was previously done for the quiescent LMXB Cen X−4 (Baglio et al. 2014a). In case of jet emission from a NS LMXB with a tangled magnetic field, one would expect to measure at most a degree of polarisation of ∼5% in the optical. If we consider our measured *i*-band polarisation upper limits (tabulated for the two sources in Tables 3 and 4), we thus obtain for the jet flux an upper limit of $(1.21\%/5) \times 100 = 24.2\%$ and $(1.97\%/5) \times 100 = 39.4\%$ of the total *i*-band flux for J1023 and J12270, respectively. These upper limits are not very constraining, meaning that the production of a jet from both systems cannot be definitely excluded by our polarimetric observations.

We then sought some clues to the production of jets by looking at the spectral energy distributions (SED) of both sources, searching for any non-thermal (flat) component in the NIR that would distort the black-body shape of the typical LMXB infrared spectrum (see for example the infrared excess in the SED of the ultra-compact X-ray binary 4U 0614+091; Migliari et al. 2010; Baglio et al. 2014b). Starting from our photometry (Sect. 5.1), we built the optical-NIR SED of the two sources, which could in principle be sufficient to detect a possible jet and to observe the frequency of the jet break. Unfortunately, we did not possess contemporaneous datasets in all of the bands. However, in the case of J1023 our group possessed a more refined photometric analysis (already published in Coti Zelati et al. 2014) that referred to an earlier epoch (end of 2013). Thanks to this analysis we obtained reliable parameters of the sinusoidal functions that describe the light curves trend in the optical. Under the hypothesis that the source did not vary considerably between 2013

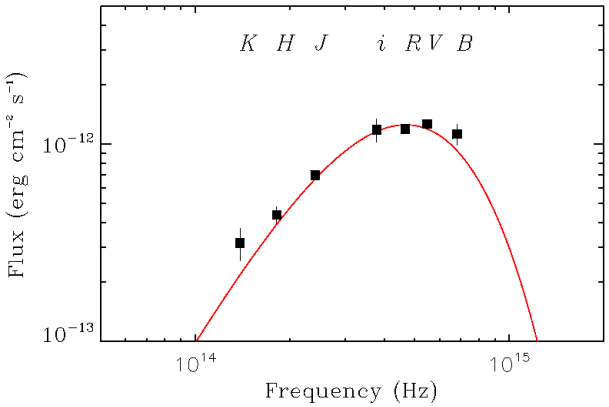

Fig. 7. NIR-optical averaged SED of J12270. Errors are indicated at the 68% confidence level. The fit of the SED with a black-body function is superimposed.

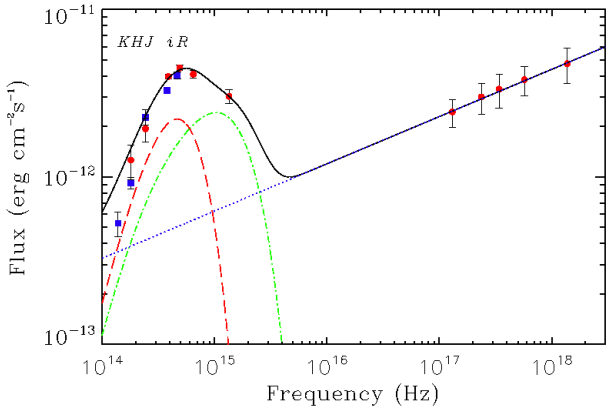

Fig. 8. NIR-optical contemporaneous SED of J1023 obtained in this work (orbital phase 0.59; blue squares); the NIR−X-rays SED of J1023 reported in Coti Zelati et al. (2014) is also represented (red dots), with superimposed the fit with a model made by the companion star (red dashed line), the accretion disc (green dash-dotted line), and the shock emission powered by the NS spin-down luminosity (blue dotted line).

and 2015, we were able to fix the semi-amplitudes of the 2015 light curves at the values reported in Coti Zelati et al. (2014) for the filters that the two works have in common (i and R) and we repeated the sinusoidal fit. In this way we gained the fluxes in the i- and R-bands at the same orbital phase as the NIR observations; we chose phase 0.59, which is the orbital phase at which the J-band data were collected.

Concerning J12270, we just built the averaged NIR−optical SED. The SEDs of the two sources are shown in Fig. 7 and are indicated with blue dots in Fig. 8.

Starting with the averaged SED of J12270, we first fixed the irradiation luminosity to the known value of the pulsar spin-down luminosity ($L_{\rm sd} = 9 \times 10^{34}$ erg s^{-1}; Roy et al. 2015). With this prior, the SED can be qualitatively well described by a simple black body of an irradiated star, where the free parameters are the radius of the star (R_*) and the fraction η of irradiation luminosity that heats the companion star. This is the case despite the poor value of the fit statistic χ^2/d.o.f. = 8.8/4, which is probably this high because the errors are underestimated. There is no need to introduce any further non-thermal component in the infrared region of the SED, which makes the production of a jet in the system strongly improbable. According to the best black-body fit, we found the fraction of irradiation luminosity that heats the donor star of the system to be $\eta = 0.32 \pm 0.05$, whereas $R_* = 0.33 \pm 0.03\,R_\odot$ (errors are indicated at the 90% c.l.); the results do not change considerably until the surface temperature of the companion star remains fixed below 4000 K in the fit.

Regarding J1023, we tried a comparison between our NIR-optical simultaneous points with the results reported in Coti Zelati et al. 2014 (referring to observations carried out in Nov. 2013; Fig. 8). J1023 appears brighter in 2015 (blue squares) than in 2013 (red dots), but this could be simply because of the different orbital phases at which observations took place (around phase 0.9 in 2013 and around phase 0.6 in 2015, i.e. nearer to the maximum of the light curve). In order to reset this effect, we applied a rigid shift of -1.05×10^{-12} erg cm^{-2} s^{-1} to the 2015 points. The best fit of the 2013 SED represented in Fig. 8 also seems to describe the optical points derived in this work well, whereas our NIR points suggest a steeper decay towards lower frequencies; the low-frequency fit of the 2013 SED, meanwhile was not as well constrained by the dataset as in 2015). Interestingly however, the $J-H$ colour measured in 2013 (0.34 ± 0.31) is consistent with that derived in 2015 (0.22 ± 0.05), which means that the components involved in the 2014 NIR emission (the black body of the irradiated companion star + the accretion disc contribution) remained almost unchanged in 2015; in particular, there is no need to introduce the emission of a jet of relativistic particles at the time of our observations to explain the observed SED. Nevertheless, Deller et al. (2015) monitored J1023 over six months in 2014 (i.e. when the source was already in its accretion phase) at radio frequencies, observing rapidly variable, but flat spectrum emission that possibly originates in an outflow from the system (or in a jet). In the epoch with the most enhanced radio activity between those reported in Deller et al. (2015) (MJD 56 674−2014, Jan. 17), the authors observed an average flux of $533 \pm 53\,\mu$Jy in the 8−12 GHz frequency range with spectral index $\alpha = -0.27 \pm 0.07$. We extended the radio flux back to the NIR to compare it with our NIR results. What we find however is that the radio predicts a lower flux than we observe, meaning that even in case of jet emission, the irradiated star (plus the accretion disc) emission is brighter than the jet itself. Therefore, it seems unlikely that the degree of polarisation observed for J1023 in our work could be actually related to the emission of a jet.

We can thus conclude that the optical LP that we measure for J1023 is more probably due to Thomson scattering with the electrons in the accretion disc rather than to synchrotron emission from a jet, since no evidence for the presence of such a phenomenon has been found in our optical and NIR photometry.

7. Conclusions

In this work we present the results of the first optical (B, V, R, i-band) polarimetric study of the two transitional pulsars PSR J1023+0038 and XSS J12270-4859, based on observations carried out on 8 and 9 February 2015 with the ESO NTT equipped with EFOSC2. In addition, we also observed both systems in the NIR on 7 February 2015 with the NTT equipped with SOFI. Whereas for J12270 the degree of optical polarisation is consistent with 0 within 3σ in all of the bands, in the case of J1023 we found a low (∼1%; Table 3), but significant, degree of polarisation in the V and R bands. The level of optical polarisation has a slight increasing trend with frequency and, in the case of the R band, this level varies (possibly sinusoidally) with the orbital phase of the system, reaching the highest value around phase 0.5, i.e. superior conjunction (when the observer sees the

irradiated face of the companion star). This peculiar behaviour is reminiscent of polarisation induced by Thomson scattering, with the free electrons that can be found in the accretion disc of the system that intercept the radiation emitted from all of the components in the system depending on the orbital phase, thus causing the observed modulation of the degree of polarisation (Fig. 4). Since we do not detect polarised light from J12270, this interpretation is also in accordance with the different states in which the two sources were lingering at the time of our observations (J1023: accretion; J12270: radio pulsar).

The measured degree of polarisation of J1023 could in principle also be ascribed to the emission of synchrotron radiation from a jet of relativistic particles. However the NIR-optical SED of J1023 is described well by the superposition of the two black bodies of the companion star and the accretion disc (Fig. 8). We do not observe a flat, non-thermal component in the NIR that could hint at the emission of synchrotron radiation from the system. This fact, together with the non-detection of a 3σ over zero degree of polarisation in the *i*-band (i.e. the band in which the jet should contribute the most in the optical regime), would suggest the real emission of a jet at the time of our observations is highly unlikely and favours our first interpretation of the measured optical polarisation. Follow-up polarimetric optical observations covering the whole orbital period of the system are strongly encouraged in order to confirm the phase-dependent oscillation of the LP.

Also, in the case of J12270, the NIR-optical SED does not suggest the emission of jets of relativistic particles and can be fitted by a black-body function of an irradiated star with radius $R_* = 0.33 \pm 0.03\,R_\odot$ and albedo (i.e. the fraction of irradiation luminosity that heats the system donor star) $\eta = 0.32 \pm 0.05$, without the need to introduce further components to the emission as expected from the polarimetric analysis.

Acknowledgements. We thank the anonymous referee for useful comments and suggestions. M.C.B. thanks George Hau, Karla Aubel, and the La Silla staff for their support during her observing run. F.C.Z. acknowledges the fruitful discussions with the international team on "The disk magnetosphere interaction around transitional ms pulsars" supported by ISSI (International Space Science Institute), Bern.

References

Alpar, M. A., Cheng, A. F., Ruderman, M. A., & Shaham, J. 1982, Nature, 300, 728
Archibald, A. M., Stairs, I. H., Ransom, S. M., et al. 2009, Science, 324, 1411
Archibald, A. M., Kaspi, V. M., Hessels, J. W. T., et al. 2013, ArXiv e-prints [arXiv:1311.5161]
Archibald, A. M., Bogdanov, S., Patruno, A., et al. 2015, ApJ, 807, 62
Baglio, M. C., D'Avanzo, P., Campana, S., & Covino, S. 2014a, A&A, 566, A9
Baglio, M. C., Mainetti, D., D'Avanzo, P., et al. 2014b, A&A, 572, A99
Bassa, C. G., Patruno, A., Hessels, J. W. T., et al. 2013, The Astronomer's Telegram, 5647
Bassa, C. G., Patruno, A., Hessels, J. W. T., et al. 2014, MNRAS, 441, 1825
Bogdanov, S., Patruno, A., Archibald, A. M., et al. 2014, ApJ, 789, 40
Bogdanov, S., Archibald, A. M., Bassa, C., et al. 2015, ApJ, 806, 148
Bond, H. E., White, R. L., Becker, R. H., & O'Brien, M. S. 2002, PASP, 114, 1359
Brown, J. C., McLean, I. S., & Emslie, A. G. 1978, A&A, 68, 415
Butters, O. W., Norton, A. J., Hakala, P., Mukai, K., & Barlow, E. J. 2008, A&A, 487, 271
Coti Zelati, F., Baglio, M. C., Campana, S., et al. 2014, MNRAS, 444, 1783
Covino, S., Molinari, E., Bruno, P., et al. 2014, Astron. Nachr., 335, 117
de Martino, D., Falanga, M., Bonnet-Bidaud, J.-M., et al. 2010, A&A, 515, A25
de Martino, D., Belloni, T., Falanga, M., et al. 2013, A&A, 550, A89
de Martino, D., Casares, J., Mason, E., et al. 2014, MNRAS, 444, 3004
de Martino, D., Papitto, A., Belloni, T., et al. 2015, MNRAS, 454, 2190
Deller, A. T., Archibald, A. M., Brisken, W. F., et al. 2012, ApJ, 756, L25
Deller, A., Degenaar, N., Hessels, J., et al. 2015, The Astronomer's Telegram, 7255, 1
di Serego Alighieri, S. 1998, in Instrumentation for Large Telescopes (Cambridge University Press), 199, 287
Dolan, J. F. 1984, A&A, 138, 1
Dolan, J. F., & Tapia, S. 1988, A&A, 202, 124
Dolan, J. F., & Tapia, S. 1989, PASP, 101, 1135
Fender, R. P. 2001, MNRAS, 322, 31
Gandhi, P., Blain, A. W., Russell, D. M., et al. 2011, ApJ, 740, L13
Gliozzi, M., Bodo, G., Ghisellini, G., Scaltriti, F., & Trussoni, E. 1998, A&A, 337, L39
Halpern, J. P., Gaidos, E., Sheffield, A., Price-Whelan, A. M., & Bogdanov, S. 2013, The Astronomer's Telegram, 5514, 1
Hill, A. B., Szostek, A., Corbel, S., et al. 2011, MNRAS, 415, 235
Jordi, K., Grebel, E. K., & Ammon, K. 2006, A&A, 460, 339
Kong, A. K. H. 2013, The Astronomer's Telegram, 5515, 1
Linares, M., Casares, J., Rodriguez-Gil, P., & Shahbaz, T. 2014, The Astronomer's Telegram, 5868, 1
Masetti, N., Morelli, L., Palazzi, E., et al. 2006, A&A, 459, 21
Migliari, S., Tomsick, J. A., Miller-Jones, J. C. A., et al. 2010, ApJ, 710, 117
Papitto, A., & Torres, D. F. 2015, ApJ, 807, 33
Papitto, A., Ferrigno, C., Bozzo, E., et al. 2013, Nature, 501, 517
Papitto, A., de Martino, D., Belloni, T. M., et al. 2015, MNRAS, 449, L26
Patruno, A., & Watts, A. L. 2012, ArXiv e-prints [arXiv:1206.2727]
Patruno, A., Archibald, A. M., Hessels, J. W. T., et al. 2014, ApJ, 781, L3
Pretorius, M. L. 2009, MNRAS, 395, 386
Radhakrishnan, V., & Srinivasan, G. 1982, Current Science, 51, 1096
Roy, J., Bhattacharyya, B., & Ray, P. S. 2014, The Astronomer's Telegram, 5890, 1
Roy, J., Ray, P. S., Bhattacharyya, B., et al. 2015, ApJ, 800, L12
Russell, D. M., & Fender, R. P. 2008, MNRAS, 387, 713
Russell, D. M., & Shahbaz, T. 2014, MNRAS, 438, 2083
Russell, D. M., Casella, P., Fender, R., et al. 2011, ArXiv e-prints [arXiv:1104.0837]
Saitou, K., Tsujimoto, M., Ebisawa, K., & Ishida, M. 2009, PASJ, 61, L13
Sazonov, S. Y., & Revnivtsev, M. G. 2004, A&A, 423, 469
Schlafly, E. F., & Finkbeiner, D. P. 2011, ApJ, 737, 103
Schmid, H. M. 2008, 2007 ESO Instrument Calibration Workshop, 499
Schultz, J., Hakala, P., & Huovelin, J. 2004, Balt. Astron., 13, 581
Serkowski, K., Mathewson, D. S., & Ford, V. L. 1975, ApJ, 196, 261
Shahbaz, T., Linares, M., Nevado, S. P., et al. 2015, MNRAS, 453, 3461
Srinivasan, G. 2010, New A Rev., 54, 93
Stappers, B. W., Archibald, A. M., Hessels, J. W. T., et al. 2014, ApJ, 790, 39
Stetson, P. B. 1987, PASP, 99, 191
Szkody, P., Fraser, O., Silvestri, N., et al. 2003, AJ, 126, 1499
Takata, J., Li, K. L., Leung, G. C. K., et al. 2014, ApJ, 785, 131
Tam, P. H. T., Kong, A. K. H., & Li, K. L. 2013, The Astronomer's Telegram, 5652
Tendulkar, S. P., Yang, C., An, H., et al. 2014, ApJ, 791, 77
Tinbergen, J. 1996, Astronomical Polarimetry (CUP)
Wardle, J. F. C., & Kronberg, P. P. 1974, ApJ, 194, 249